

where  $\beta = 2k_{\text{F}}R$  and  $\alpha = 2k_{\text{F}}\gamma$ .

At large  $R$ ,  $F_{\gamma}$  and  $F$  do not differ greatly for small  $\gamma$ . However, for small  $R$ ,  $F_{\gamma}$  achieves a finite value while  $F$  has a singularity at  $R = 0$ . The consequences of the differences between  $F_{\gamma}$  and  $F$ , and other effects of phonons on the model, will be discussed elsewhere.<sup>5</sup>

Figure 1 shows a comparison of  $F_{\gamma}$  and  $F$  for small  $R$  and the values  $2k_{\text{F}}\gamma = 1$  and  $2k_{\text{F}}\gamma = 0$ .

As a final point, the relationship between the VC divergences and the Kondo singularity<sup>6</sup> in the resistivity should be clarified. Calculation of the Kondo terms in resistivity with the effective Hamiltonian in Eq. (3) alters Kondo's results only by a multiplicative factor

$$2\{1 - \exp[-\frac{1}{2}(2k_{\text{F}}\gamma)^2]\}/(2k_{\text{F}}\gamma)^2$$

which approaches 1 as  $\gamma \rightarrow 0$ . The VC divergenc-

es arose from large momentum transfers while Kondo's singularity involves small energy and momentum transfers near the Fermi surface.

The author would like to thank Professor C. Kittel for suggesting this problem and for several helpful discussions.

\*Work assisted by the National Science Foundation.

<sup>1</sup>G. Vertogen and W. J. Caspers, *Z. Physik* **198**, 37 (1966), hereafter referred to as VC.

<sup>2</sup>The second-order calculation of the indirect interaction is called the Ruderman-Kittel-Kasuya-Yosida (RKKY) interaction; M. A. Ruderman and C. Kittel, *Phys. Rev.* **96**, 99 (1954); K. Yosida, *Phys. Rev.* **106**, 893 (1957).

<sup>3</sup>This function is written as Eq. (4) of this Letter, or see Ruderman and Kittel and Yosida, Ref. 2.

<sup>4</sup>See particularly Eq. (25c) and Eq. (28) of Ref. 1.

<sup>5</sup>S. P. Bowen, to be published.

<sup>6</sup>J. Kondo, *Progr. Theoret. Phys.* **32**, 37 (1954).

## RESONANCE FREQUENCIES OF THE ORTHOFERRITES IN THE SPIN REORIENTATION REGION\*

J. R. Shane

Sperry Rand Research Center, Sudbury, Massachusetts

(Received 21 February 1968)

The purpose of this Letter is to present a theory of the resonance modes of a canted, orthorhombic antiferromagnet in the temperature region where the  $a$ - $c$  plane anisotropy changes sign. The results are applied to the rare-earth orthoferrites in which the direction of the weak moment changes from the  $a$  axis to the  $c$  axis with increasing temperature.<sup>1-4</sup> It is found that low-frequency antiferromagnetic resonance modes occur in the reorientation region.

The theoretical results provide an interpretation for recent microwave absorption measurements<sup>5</sup> which have not been adequately explained. The results show that resonant absorptions should be observed at zero applied field for a wide range of frequencies. Additional results of the theory, also verified experimentally, include the fields for resonance along the  $a$  and  $c$  axes, the directions of maximum rf susceptibility, and the angular dependence of the resonance amplitude.

A two-sublattice model has been used to calculate the equilibrium position of the magnetization vectors and the resonance frequencies. The model is similar to the one used by Herr-

mann,<sup>6</sup> but has been extended to include the effects of fourfold anisotropy terms which are important in the region considered. A preliminary analysis<sup>5</sup> suggests that the relatively low resonance frequencies implied by Herrmann's results are eliminated when fourfold terms are included. However, it is shown here that if the fourfold anisotropy is consistently taken into account in the expressions for the equilibrium configurations and the resonance frequencies, then low-frequency modes are predicted by this model.

The energy expression for the model contains the following terms:

$$E = MH_E(\vec{m}_1 \cdot \vec{m}_2) + M\vec{H}_D \cdot (\vec{m}_1 \times \vec{m}_2) - M\vec{H}_0 \cdot (\vec{m}_1 + \vec{m}_2) + E_A \quad (1)$$

Here,  $\vec{m}_1$  and  $\vec{m}_2$  are unit vectors in the directions of the sublattice moments,  $M$  is the magnitude of the moments,  $H_E$  is the isotropic exchange field, and  $H_0$  is the applied field. The antisymmetric exchange field  $\vec{H}_D$  is directed along the  $b$  axis. The anisotropy energy

$E_A$  is assumed to have the form

$$E_A/M = -\frac{1}{2}H_1(m_{1x}^2 + m_{2x}^2) - \frac{1}{2}H_3(m_{1z}^2 + m_{2z}^2) + \frac{3}{8}H_4 \sum_{i=1,2} m_i \alpha^4 - H_C(m_{1x}m_{1z} - m_{2x}m_{2z}), \quad (2)$$

$$\alpha = x, y, z$$

where  $H_1$  and  $H_3$  refer to effective fields along the  $a$  and  $c$  axes, respectively. The effective field  $H_4$  is the coefficient of the fourfold terms,  $H_C$  is the single-ion canting field, and the subscripts  $[x, y, z]$  refer to the  $a, b, c$  axes.

There are four angular variables in the problem; by minimizing  $E$  with respect to three of these, we obtain from Eq. (1) an energy expression for applied-field orientations in the  $a$ - $c$  plane:

$$F = -H_0^2 \cos^2(\theta - \theta_0) - 2H_0 \cos(\theta - \theta_0)[H_D + H_C \cos 2\theta_0] - \frac{1}{2}[2H_E(H_1 - H_3) + 4H_D H_C] \cos 2\theta_0 + \frac{1}{8}[3H_E H_4 - 4H_C^2](\cos 4\theta_0 - 1), \quad (3)$$

where  $\theta_0$  is the angle between the weak moment and the  $c$  axis, and  $\theta$  specifies the applied-field orientation. In obtaining Eq. (3), we have neglected terms of order  $\sim H_E(H_1 - H_3)\delta^2$  and  $H_E H_4 \delta^2$ , where  $\delta$  is the canting angle. Also, it has been assumed that  $H_1$  and  $H_3$  are positive and  $H_D > H_C$ ; otherwise, additional solutions must be considered. With  $H_0 = 0$ , the stationary values of  $F$  are given by

$$(\cos 2\theta_0 - \tau) \sin 2\theta_0 = 0, \quad (4)$$

where  $\tau$  is the ratio of the coefficients of the twofold to fourfold terms,

$$\tau = \frac{2H_E(H_1 - H_3) + 4H_D H_C}{3H_E H_4 - 4H_C^2}. \quad (5)$$

The solutions of Eq. (4) given by  $\cos \theta_0 = 0$  and  $\sin \theta_0 = 0$  correspond to Herrmann's configurations II and IV, respectively.<sup>6</sup> For systems in which  $H_1 - H_3$  changes sign as a function of temperature, we define the temperatures  $T_l$  and  $T_h$ , such that  $\tau(T_l) = -1$  and  $\tau(T_h) = +1$ ; then additional solutions exist for  $T_l < T < T_h$ , given by  $\cos 2\theta_0 = \tau$ . The configurations which correspond to  $\sin \theta_0 = 0$ ,  $\cos \theta_0 = 0$ , and  $\cos 2\theta_0 = \tau$  are shown in Fig. 1.

If  $3H_E H_4 - 4H_C^2 > 0$ , the solutions of  $\cos 2\theta_0 = \tau$  are stable and the spin reorientation takes

place continuously as a function of temperature. This is consistent with recent torque and magnetization measurements.<sup>4</sup> The stationary values of  $F(H_0 = 0)$  are shown in the upper half of Fig. 1 as functions of the parameter  $\tau$ . The solid and dashed lines correspond to stable and unstable regions, respectively. At a temperature  $T_c$  such that  $\tau(T_c) = 0$ , then  $\sin \theta_0 = \pm 1/\sqrt{2}$ . This is the temperature at which  $2H_E(H_1 - H_3) + 4H_D H_C = 0$ , and it can be noted from Eq. (3) that, for  $H_0 = 0$ , the energy contains only fourfold terms. This is also consistent with recent measurements of torque versus applied-field orientation which show fourfold symmetry when the weak moment is  $45^\circ$  from the  $c$  axis.<sup>4</sup>

If  $3H_E H_4 - 4H_C^2 < 0$ , the solutions,  $\cos 2\theta_0 = \tau$ , are free-energy maxima. For this case, configuration II would be unstable above  $T_h$  and configuration IV would be unstable below  $T_l$ ; in between, both states would be locally stable. The spin reorientation would be a first-order phase transition with the possibility of hysteresis effects occurring. This has not been observed experimentally, so the following description of the resonances will be confined to the case in which  $3H_E H_4 - 4H_C^2 > 0$ .

For applied fields in the  $a$ - $c$  plane, the exact solutions for the resonance frequencies are given by

$$(\omega/\gamma)^4 - 2(\omega/\gamma)^2(H_1^+ H_2^+ + H_1^- H_2^- + H_E^2 g^2) + [(H_1^+)^2 - (H_1^-)^2 - H_E^2] [(H_2^+)^2 - (H_2^-)^2 - H_E^2 g^2] = 0, \quad (6)$$

where

$$H_E g = -H_E \cos 2\delta + \vec{H}_D \cdot (\vec{m}_1 \times \vec{m}_2),$$

$$H_{1,2}^+ = -H_E g + \frac{1}{2} \vec{H}_0 \cdot (\vec{m}_1 + \vec{m}_2) + h_{1,2}^+, \quad H_{1,2}^- = \frac{1}{2} \vec{H}_0 \cdot (\vec{m}_1 - \vec{m}_2) + h_{1,2}^-,$$

and

$$-2Mh_{i=1,2}^{\pm} = \sum_{\alpha} \left[ R_{3\alpha} + \frac{\partial E_A}{\partial m_{1\alpha}} \pm R_{3\alpha} - \frac{\partial E_A}{\partial m_{2\alpha}} \right] - \sum_{\alpha, \beta} \left[ R_{i\alpha} + R_{i\beta} + \frac{\partial^2 E_A}{\partial m_{1\alpha} \partial m_{1\beta}} \pm R_{i\alpha} - R_{i\beta} - \frac{\partial^2 E_A}{\partial m_{2\alpha} \partial m_{2\beta}} \right].$$

The indices  $\alpha, \beta$  run over  $x, y, z$ ; the matrices  $R^+$  and  $R^-$  transform the  $[x, y, z]$  coordinate system to coordinates fixed on the equilibrium positions of  $\bar{m}_1$  and  $\bar{m}_2$ :

$$R^{\pm} = \begin{bmatrix} 0 & 1 & 0 \\ \pm \sin(\theta_0 \mp \delta) & 0 & \pm \cos(\theta_0 \mp \delta) \\ \pm \cos(\theta_0 \mp \delta) & 0 & \mp \sin(\theta_0 \mp \delta) \end{bmatrix}.$$

Computer programs were used to solve the equilibrium equations and evaluate the resonance frequencies<sup>7</sup> for typical values<sup>8</sup> of the

internal fields for the orthoferrites. The zero-field frequency of the lower mode is shown in the lower half of Fig. 1 as a function of  $\tau$ . The following values in Gauss were used:  $H_E = 10^7$ ,  $H_D = 2 \times 10^5$ ,  $H_1 = 2 \times 10^3$ ,  $H_C = 10^3$ , and  $H_4 = 40$ . The value of  $H_4$  was estimated<sup>9</sup> from the torque measurements of Ref. 4 for  $\text{SmFeO}_3$ .  $H_C$  was assumed to be the same order of magnitude as  $H_1$  and  $H_3$ . The parameter  $\tau$  was varied by letting  $H_3$  have values from 2.19 kG for  $\tau = -2.5$  to  $H_3 = 1.92$  kG for  $\tau = 2.0$ .

In Fig. 1 it is shown that the lower frequency mode moves rapidly to zero near  $T_l$  and  $T_h$ . This can be understood by considering the shape of the anisotropy surface near  $\tau = 1$ . At  $\tau = 1 - \Delta$ , the energy surface has a maximum at  $\sin \theta_0 = 0$  and minima on each side at  $\sin \theta_0 = \pm (\frac{1}{2}\Delta)^{1/2}$ . As  $\tau$  approaches 1, the stationary values converge in such a manner that the energy surface is locally flat at  $\theta_0 = 0$ , and no restoring torques exist for small displacements of the sublattice moments in the  $a$ - $c$  plane. Since the twofold terms are zero at  $\tau = 0$ , the maximum frequency  $\nu_m$ , which occurs at the center of the spin reorientation region, is determined by the magnitude of the fourfold terms.

Experimentally,<sup>1,4</sup> the width of the reorientation region,  $T_h - T_l$ , is 10 to 20°K. If the linewidths are such that absorptions are observed over a 1°K temperature interval, the splitting of the lines at low frequencies would not be resolved. Resonances should be observed near  $T_l$  and  $T_h$ , independent of the operating frequency, for frequencies small compared with  $\nu_m$ . The experiments in  $\text{TmFeO}_3$  have shown absorption peaks ranging from 0.37 to 2°K wide, which occurred at  $T_l$  and  $T_h$  at frequencies ranging from 5 MHz to 54 GHz.<sup>5</sup> This is qualitatively consistent with the model presented here. Quantitatively, the fact that measurements were performed as high as 54 GHz and a splitting of the lines was not reported<sup>10</sup> probably indicates that for  $\text{TmFeO}_3$ ,  $H_4$  is larger than the value assumed in the calculation summarized by Fig. 1. An estimate of  $H_4$  as well as other internal fields in  $\text{TmFeO}_3$ , based on the data of Ref. 5, will be made after the effects of applied fields on the resonance have been described.

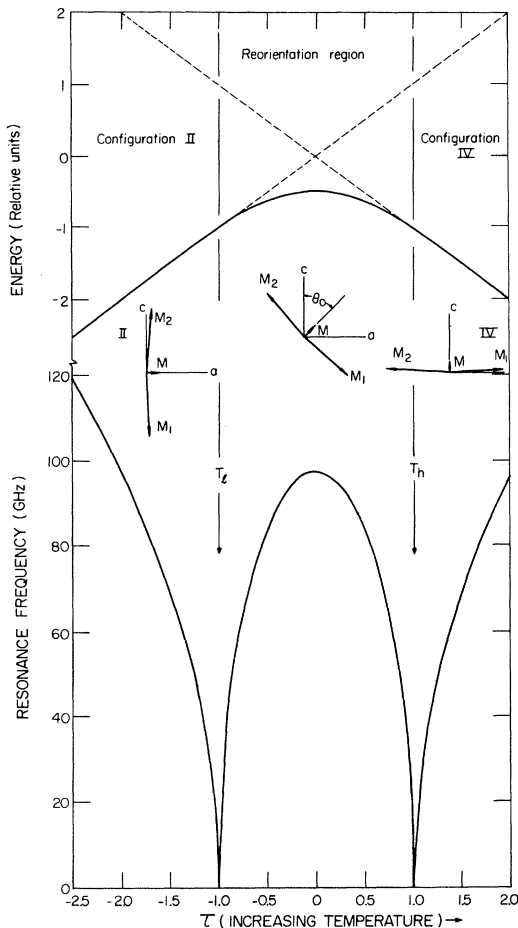


FIG. 1. The energies of the spin configurations are shown in the upper portion of this figure; the stable configuration for the different temperature regions is shown in the center; the frequency of the lower resonance mode as a function of the parameter  $\tau$  for  $H_0 = 0$  is shown in the lower portion.

With an applied field along the  $c$  axis, the equilibrium configurations are obtained from Eq. (3) with  $\theta=0$ . The solutions are given by  $\sin\theta_0=0$ , and a cubic equation for  $\cos\theta_0$ . For  $T>T_h$ , the stable solution is  $\sin\theta_0=0$  (configuration IV) for all values of the applied field. For  $T_l < T < T_h$ , the stable solution for low applied fields is that root of the cubic equation which reduces to  $\cos\theta_0 = [\frac{1}{2}(1+\tau)]^{1/2}$  at  $H_0=0$ . For  $T < T_l$ , the stable configuration is given by the only real root of the cubic equation; it reduces to  $\theta_0 = \frac{1}{2}\pi$  (configuration II) at  $H_0=0$ . These last two solutions ( $T < T_h$ ) no longer exist for applied fields greater than  $H_{cr}^c$ , the critical field just required to pull the weak moment to the  $c$  axis:

$$H_{cr}^c = -\frac{1}{2}(H_D + 4H_C) + \left\{ \left[ \frac{1}{2}(H_D + 5H_C) \right]^2 + (3H_E H_4 - 4H_C^2)(1-\tau) \right\}^{1/2}. \quad (7)$$

The resonance frequency of the lower mode for  $\theta_0=0$  is approximately given by

$$(\omega/\gamma)^2 = H_0^2 + H_0(H_D + 5H_C) + (3H_E H_4 - 4H_C^2)(\tau-1) \quad (8)$$

which goes to zero at  $H_0 = H_{cr}^c$  for  $\tau < 1$ .

It should be remarked here that the approximations used in writing the above equations are a matter of convenience. The exact result corresponding to Eq. (8) has the form

$$(\omega/\gamma)^2 = (h_2^+ + H_0 \sin\delta)(H_E + H_1^+) \quad (9)$$

and the exact equilibrium equations require that

$$h_2^+ + H_0 \sin\delta = 0 \text{ for } H_0 = H_{cr}^c, \tau < 1 \\ \text{and } H_0 = 0, \tau = 1. \quad (10)$$

The resonance frequency of the lower mode is shown in Fig. 2 as a function of applied field for several values of  $\tau$ . The internal field values are the same as those used in the calculations for Fig. 1. The results show that the resonance can be tuned from zero to over 100 GHz with only moderate applied fields. For similar linewidth considerations as discussed above, resonances should be observed below  $T_h$  at  $H_0 \approx H_{cr}^c$ , independent of the operating frequency for frequencies small compared with  $\nu_m$ . The  $a$  axis is the direction of maximum

rf susceptibility for this resonance.

The situation just described is only slightly changed by small angular displacements,  $\epsilon$ , of the applied field away from the  $c$  axis in the  $b$ - $c$  plane. Although the weak moment is no longer pulled exactly parallel to the  $c$  axis, it is found that stationary values of the energy form a double root which gives zero frequencies for  $T < T_h$  at  $H_0 = H_{cr}'$ , the field just required to pull the vector  $\vec{m}_1 - \vec{m}_2$  parallel to the  $a$  axis. To a good approximation, we find  $H_{cr}' = H_{cr}^c (\cos\epsilon)^{-1}$  which only changes in second order with  $\epsilon$  for small displacements.

For small components of  $H_0$  parallel to the  $a$  axis, the situation is quite different. The resonance no longer goes to zero, and the minimum near  $H_0 = H_{cr}^c$  moves rapidly to higher frequencies with increasing applied field components parallel to the  $a$  axis. This effect should appear experimentally as a sharp decrease in the resonance amplitude as the minimum resonance frequency moves above the operating frequency.

Similar resonances occur with the applied field along the  $a$  axis. For  $T > T_l$ , the frequency of the lower mode moves rapidly to zero at  $H_0 = H_{cr}^a$ , the field required to stabilize configuration II. For operating frequencies small compared with  $\nu_m$ , resonances should be observed at

$$H_{cr}^a = -\frac{1}{2}(H_D - 5H_C) + \left\{ \left[ \frac{1}{2}(H_D - 5H_C) \right]^2 + (3H_E H_4 - 4H_C^2)(1+\tau) \right\}^{1/2}. \quad (11)$$

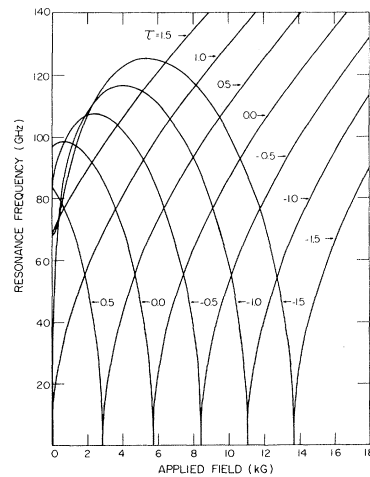


FIG. 2. Frequency of the lower resonance mode as a function of applied field for several values of the parameter  $\tau$ .

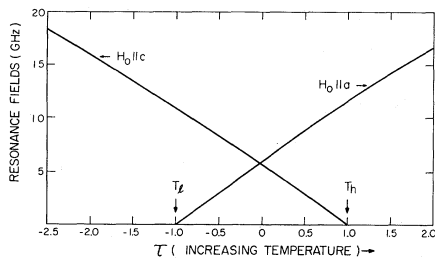


FIG. 3. Fields for resonance parallel to the  $a$  and  $c$  axes for frequencies small compared with  $\nu_m$ .

The direction of maximum rf susceptibility for this resonance is the  $c$  axis.

The absorption peaks<sup>5</sup> in  $\text{TmFeO}_3$  displayed all of the characteristics of the resonances described above. The data are schematically reproduced in Fig. 3 by showing Eqs. (7) and (11) as functions of the parameter  $\tau$ .

The relative magnitudes of the two types of canting fields can be determined from the curves in Fig. 3:

$$H_C \approx \frac{H}{5}(\tau-1)/(\tau+1)H_D, \quad (12)$$

where  $-\tau$  is the ratio of the slopes of the two curves, and it has been assumed that  $H_0 \ll H_D \pm 5H_C$ . From the data of Ref. 5 we obtain  $H_C \approx 0.09H_D$  for  $\text{TmFeO}_3$ . This should be compared with the result of Ref. 4,  $H_C \approx 0.3H_D$ , obtained by measuring the change in canting angle from  $T_l$  to  $T_h$ . Reasons for this disagreement will be discussed elsewhere.<sup>11</sup> However, if  $H_C$  were as large as  $0.3H_D$ , Eq. (11) shows that applied fields greater than  $0.5H_D$  would be required to pull the weak moment parallel to the  $a$  axis for  $T > T_l$ . This is inconsistent with the experimental results of Ref. 5.

Finally, from Eqs. (7) and (12) and the value of  $H_{Cr}^C$  at  $T = T_l$ , the magnitude of the four-

fold anisotropy field can be determined if  $H_E$  and  $H_D$  are known. Using  $H_C \approx 0.09H_D$ ,  $H_E \approx 10^7$  G, and  $H_D \approx 2 \times 10^5$  G, we obtain from the data<sup>5</sup>  $H_4 \approx 80$  G for  $\text{TmFeO}_3$ .

\*The research reported in this paper was supported in part by the U. S. Air Force Cambridge Research Laboratories, Office of Aerospace Research, under Contract No. AF 19628-67-C-0346, but does not necessarily reflect endorsement by the sponsor.

<sup>1</sup>R. M. Bozorth, V. Kramer, and J. P. Remeika, Phys. Rev. Letters **1**, 3 (1958).

<sup>2</sup>C. Kuroda, T. Miyadai, A. Naemura, N. Niizeki, and H. Takata, Phys. Rev. **122**, 446 (1961).

<sup>3</sup>D. Treves, J. Appl. Phys. **36**, 1033 (1965), and Phys. Rev. **125**, 1843 (1962).

<sup>4</sup>E. M. Gyorgy, J. P. Remeika, and F. B. Hagedorn, in Proceedings of the International Congress on Magnetism, Boston, Massachusetts, 11-15 September 1967 (to be published).

<sup>5</sup>R. C. LeCraw, R. Wolfe, E. M. Gyorgy, F. B. Hagedorn, J. C. Hensel, and J. P. Remeika, in Proceedings of the International Congress on Magnetism, Boston, Massachusetts, 11-15 September 1967 (to be published).

<sup>6</sup>G. F. Herrmann, Phys. Rev. **133**, A1334 (1964), and J. Phys. Chem. Solids **24**, 597 (1963).

<sup>7</sup>For the internal fields assumed, the higher frequency is 791 GHz at  $\tau=0$  and changes by less than 2% for the values of  $\tau$  and  $H_0$  used here.

<sup>8</sup>The magnitudes of  $H_E$  and  $H_D$  are reasonably constant for the orthoferrites (Ref. 3). Although  $H_1$  and  $H_3$  may vary considerably from one compound to another, only the difference  $H_1 - H_3$  is important for the lower resonance frequency.

<sup>9</sup>The anisotropy constant  $K_b$  of Ref. 4 is related to the parameters of the model presented here by  $K_b = (M/16H_E)[3H_E H_4 - 4H_C^2]$ .

<sup>10</sup>The usual phase relationship between the real and imaginary parts of the susceptibility for resonance absorptions was not observed (Ref. 5). This effect may be caused by the superposition of the unresolved lines.

<sup>11</sup>J. R. Shane, to be published.

#### INFLUENCE OF THE KONDO SCATTERING ON THE AMPLITUDE OF THE de HAAS-van ALPHEN OSCILLATIONS\*

B. E. Paton† and W. B. Muir

Eaton Electronics Research Laboratory, McGill University, Montreal, Quebec, Canada

(Received 26 February 1968)

The anomalous amplitude of the de Haas-van Alphen oscillations observed in an alloy exhibiting the Kondo effect<sup>1</sup> has been explained on the basis of a simple square-well energy-dependent conduction-electron relaxation time. Recently the  $s$ - $d$  scattering theory of Kondo<sup>2</sup> has given an explicit expression for the ener-

gy dependence of the relaxation time which is consistent with the observed resistance minimum. In the present Letter we wish to examine the influence of Kondo scattering on the de Haas-van Alphen effect and to reinterpret the earlier data on the Zn-Mn system.

The relaxation time  $\tau$  for an electron in a